A 350 MHz, 200 kW CW, Multiple Beam IOT

U.S. Department of Energy Grant DE-FG-3-07ER84876

Calabazas Creek Research, Inc.
690 Port Drive
San Mateo, CA 94404
(650) 312-9575
RLI@CalCreek.com

December 31, 2011

1. Introduction

This program was tasked with developing a 350 MHz, 200 kW multiple beam inductive output tube (MBIOT). The specifications are indicated in Table 1.

Table 1. MBIOT Specifications

Parameter	Value
Frequency	350 MHz
Bandwidth	4 MHz
Output Power	200 kW CW
Gain	23 dB
Operating Voltage	30 kV
Efficiency	70%
Total Current	9.5 A
Number of Beams	7
Average current per beam	1.4 A

The design was finalized during the first year of the program (8/1/08 - 7/31/09), and the drawings and mechanical design were completed during the first months of the second year. The electron guns were ordered in January 2009, with delivery indicated as June 2009. Unfortunately, issues with grid fabrication delayed the delivery of the electron guns. The electron guns were finally received in November 2010, which dramatically delayed assembly of the IOT,

All other parts for the tube were received early in 2011. The last parts to arrive were the copper and iron plates comprising the end plate assembiles for the output cavity. Failure ot the vendor to machine these plates to specifications also delayed the assembly.

Because of these vendor delays, CCR could not complete the assembly of the MBIOT prior to the end of the Phase II program. CCR is continuing this assembly, and testing is scheduled for spring 2012 at Argonne National Laboratory.

This report summarized the design and current status of major subassemblies.

2. Design

2.1. Input Cavity and Electron Gun

The design utilizes an existing production electron gun produced by Communications & Power Industries, Inc. (CPI). These guns were developed several years ago and are implemented in all commercial IOTs produced by CPI. Consequently, their performance is well documented. Figure 1 shows a photograph of the K2 gun. It uses a pyrolytic graphite grid driven by the input cavity to generate the modulated electron beam from the cathode.

Seven guns are arranged in a circular pattern to drive a fundamental mode output cavity. The number of beams was selected to provide an operating voltage of 30 kV.

The principal challenge in the progrem was design of the input cavity. The input cavity must receive the input RF signal and drive all seven guns in phase at the RF frequency. As shown in Figure 2, the input cavity is a coaxial structure with the electron guns arranged around the periphery. The principal design code for the input cavity was Ansoft's High Frequency Structure Simulator (HFSS). HFSS modeled the input RF signal and fields produced at the cathode surface by the grid. Figure 3 shows the HFSS model, including the input waveguide and step transducer for matching to the input cavity

Figure 1. Photograph of CPI K2 gun

.

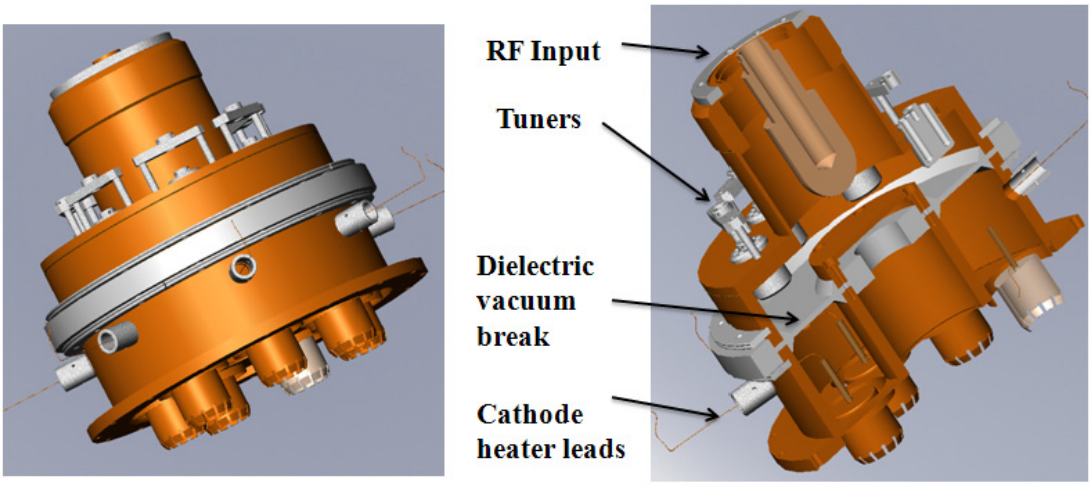

Figure 2. Solid model of the MBIOT input cavity

Figure 3. HFSS model of the input cavity, including the input waveguide and transducer

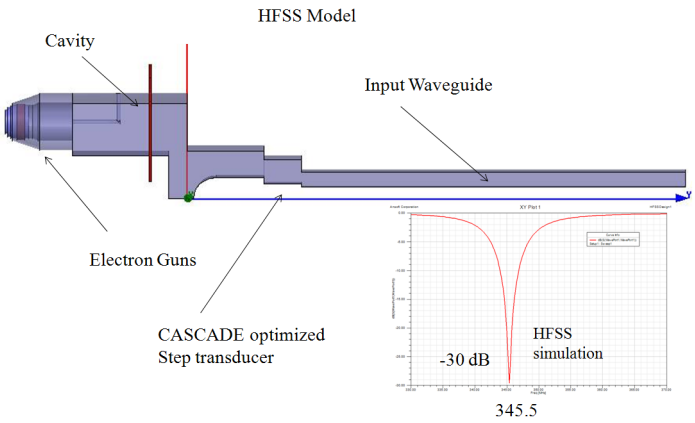

Figure 4 shows the electric fields produced in the cavity during one phase of the RF cycle. The electron gun is on the extreme left with the input waveguide to the right. The electrical power for the cathode heater is brought in radially from the periphery of the input cavity. The vertical red structure near the center represents a DC break to isolate the grounded input from the electron gun at 30 kV. The input cavity operates at atmospheric pressure. The vacuum seal for the electron gun is contained within the gun structure.

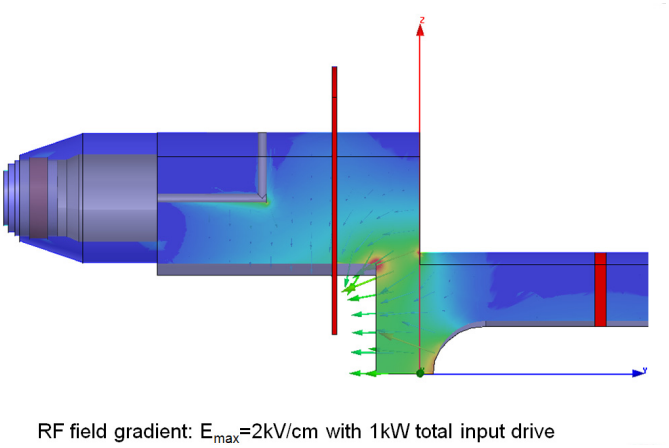

Figure 4. HFSS simulation of the input cavity electric fields at one phase of the RF cycle

Tuners will be positioned behind each electron gun to adjust the frequency and coupling to precisely balance the electric fields for each electron gun. Figure 5 shows the location of the tuners.

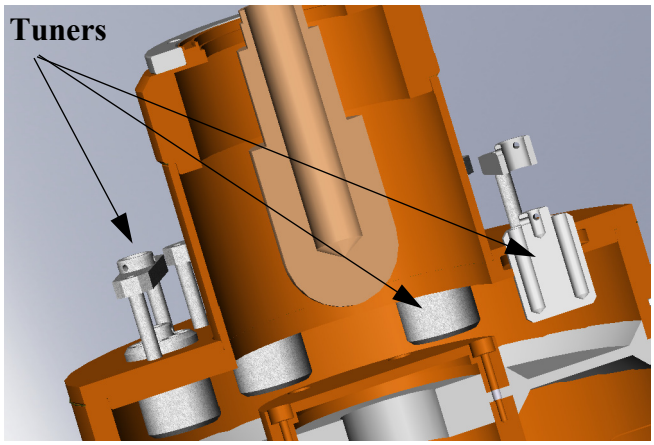

Figure 5. Input cavity tuners

The electron beam optics design utilized a number of computational codes, including the trajectory codes TRAK, Omni-TRAK, and Beam Optics Analyzer (BOA). Because the device uses multiple guns displaced from the IOT axis, 3D simulation was required. IOTs use an electron beam modulated at the RF frequency, so a time domain code is required to verify proper operation. CCR used MAGIC to analyze the time dependent performance. Figure 6 shows plots from the beam simulation. The bottom simulation confirms complete transmission of the beam through the output cavity and into the collector. Beam quality in an IOT is necessarily lower than in a normal device, as the current in the beam is a function of the phase of the RF cycle. Optimum performance can only be achieved at one phase of the cycle. Simulations were performed at different phases to verify beam transmission under all operating conditions.

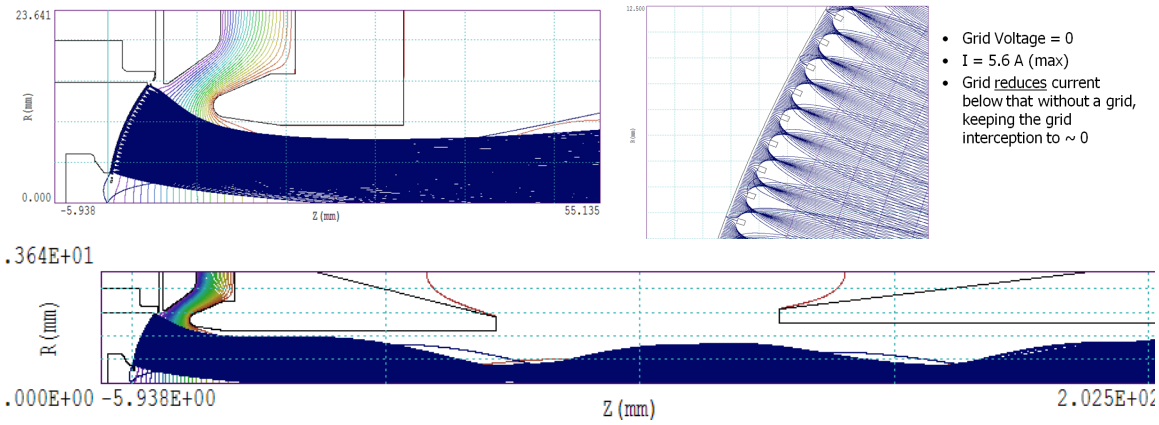

Figure 6. Plots from simulations of the electron gun. The top right is a simulation of the beam into the output cavity. The top right shows the trajectories near the grid. The bottom image confirms transmission through the output cavity and into the collector. All simulations are at one phase of the RF cycle.

2.2. Output Cavity

Design of the output cavity was relatively straight forward, since it is a fundamental mode cavity. Consequently, parasitic modes are not an issue. The primary challenge was determining the appropriate impedance for the seven electron beams, given their number and radial position. The fields were modeled using HFSS, and the impedance determined by integrating the current in the fields for a single beam. Figure 7shows a sliced solid model of the output cavity. The RF output is along the device axis and passes through the coaxial collector, described later. The position of the inner coax conductor will be

Figure 7. Output cavity geometry. Images of the HFSS geometry are shown on the right.

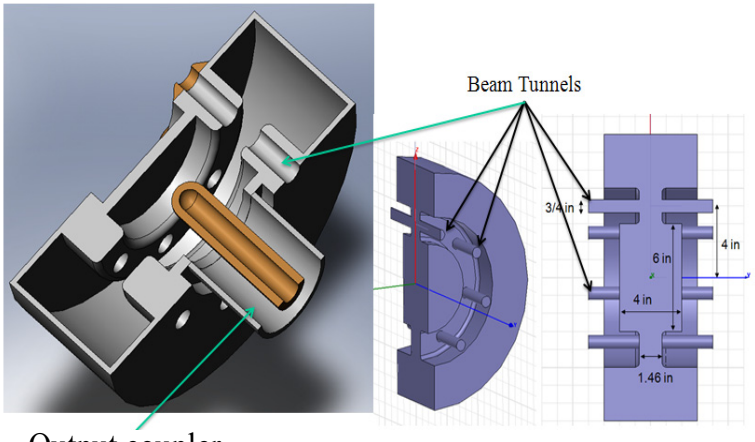

adjustable to allow tuning the cavity quality factor (Q) and coupling. Figure 8 shows HFSS simulation of the electric fields. These simulation indicated the fields are properly positioned for interaction with the electron beams and that surfaces will not break down during operation. Figure 9 shows a plot of the output coupling.

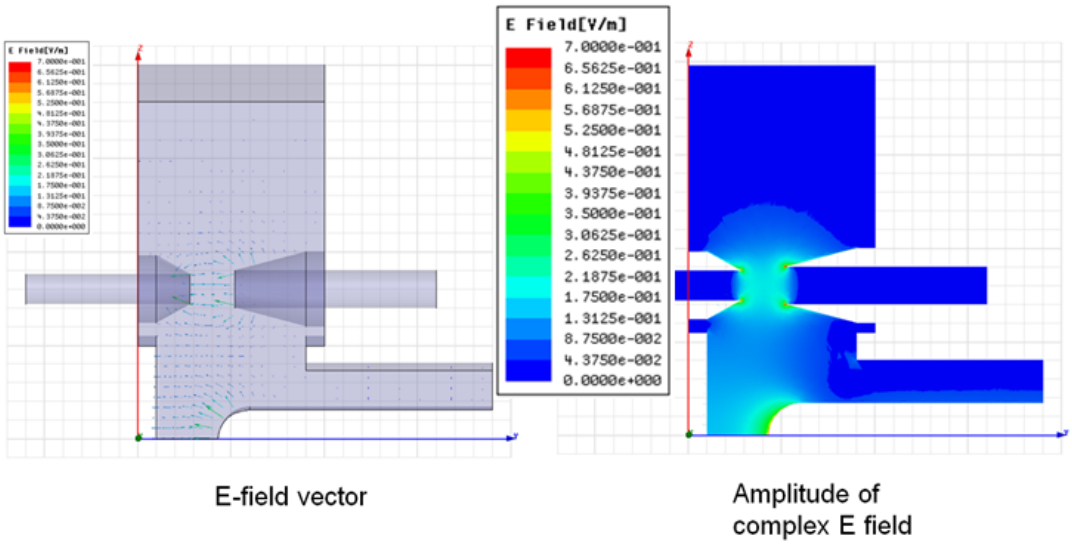

Figure 8. HFSS simulation of electric fields in the output cavity

Output cavity parameters are summarized in the following table.

Table 2. Output Cavity Parameters

Parameter	Value	Parameter	Value
Freq (MHz)	350	Q_o	10,000
Output Power (kW)	200	E_{max} (kV/cm) at drift tube tip (0.02" radius)	40
Gap Voltage (kV)	26	E_{max} (kV/cm) at tip of output coax	30
Stored Energy (mJ)	3.64	E_{max} (kV/cm) on coax inner conductor	2.3
R/Q	303	Loss density on coax inner conductor (W/cm^2)	0.18
Q_e	40	Per unit length power deposit on inner coax (W/in)	6.2

Both the input and output RF signals are transmitted in coaxial waveguide. No window is required on the input, as the input cavity operates at atmospheric pressure. The output window, however, must provide a high vacuum boundary and transmit 200 kW of continuous RF power. The window was thoroughly analyzed for thermal and mechanical performance using the code ANSYS. The analysis provided guidance on materials and water cooling requirements on the inner coaxial conductor through the window ceramic (alumina Al-995). Figure 10 shows a sliced solid model of the output window.

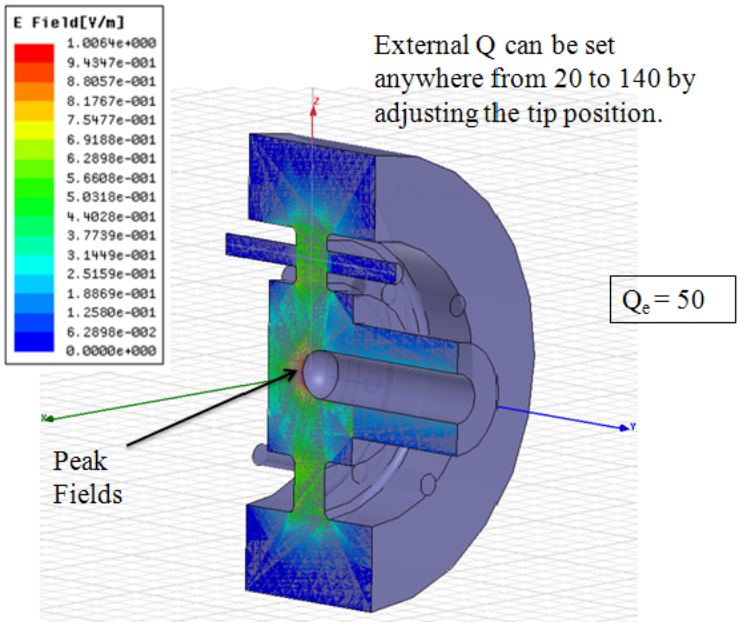

Figure 9. HFSS simulation of the output coupling

2.3. Collector

The collector receives the electron beam after transmission through the output cavity and dissipates the remaining power. The multiple beam geometry required 3D simulation of the electron trajectories to determine the power distribution. CCR used this information to thermally analyze the geometry and determine the configuration and cooling requirements. Figure 11 shows the geometry of the collector, including the output waveguide and portions of the output cavity. Figure 12 shows several images of the beam distribution in the collector.

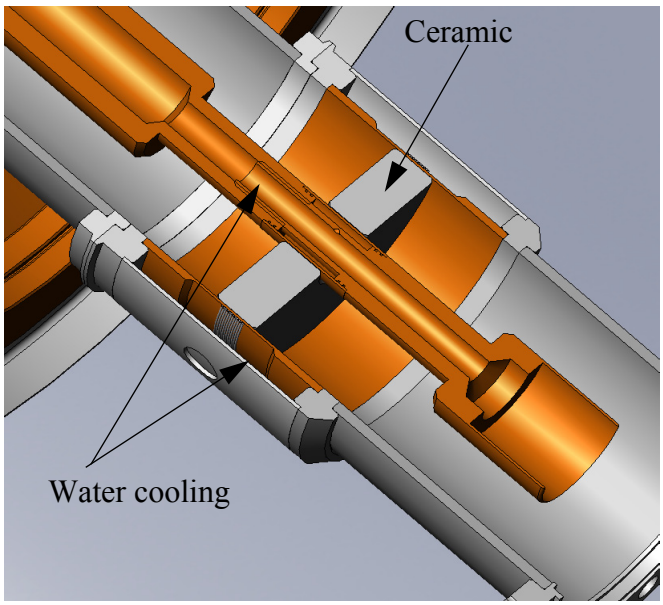

Figure 10. Sliced solid model of the output window

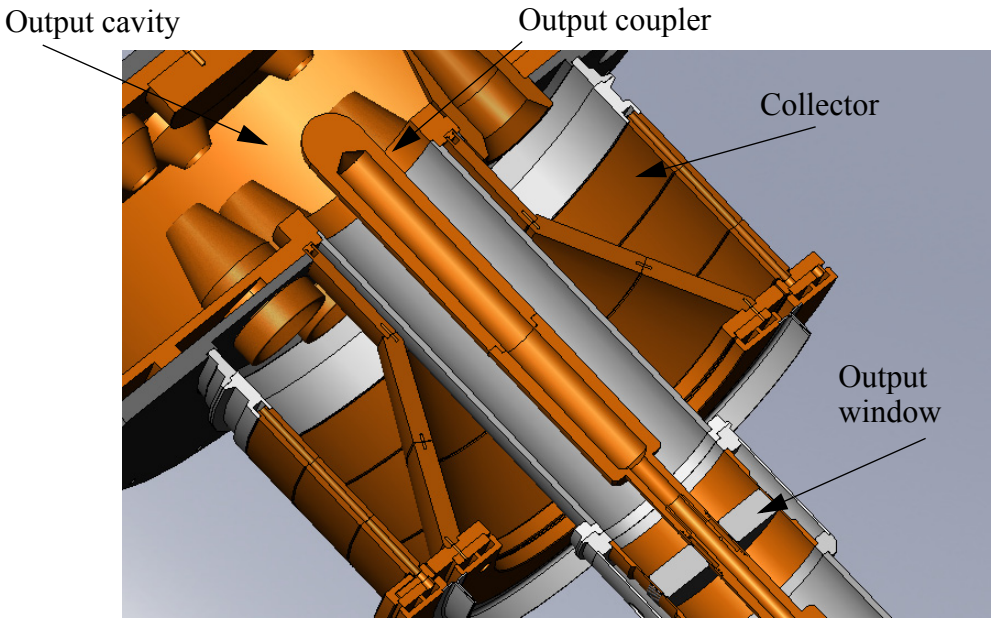

Figure 11. MBIOT collector model

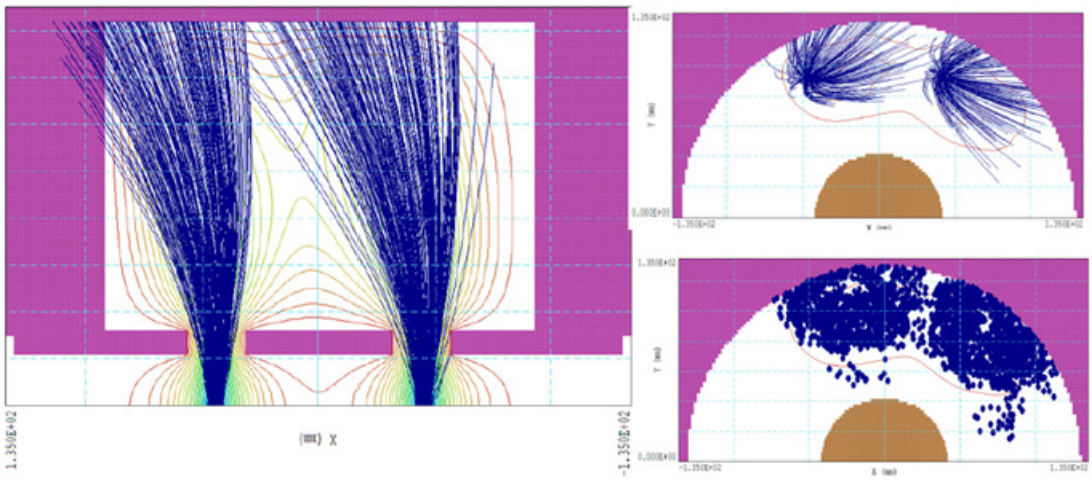

Figure 12. Beam simulations in the collector. Left image is 'unrolled' simulation of two adjacent electron beams. Right images are radial views of trajectories (top) and particles (bottom)

2.4. Mechanical Design

Figure 13 shows the total layout drawing of the MBIOT with a simulated 6 ft. tall person. This provides information on the total size and configuration of the device. In the right image, the RF input is at the top and the output is at the bottom. The gray region around the midsection is the iron shield enclosing the solenoid. The structure at the top is a stub tuner for matching the input signal into the input cavity.

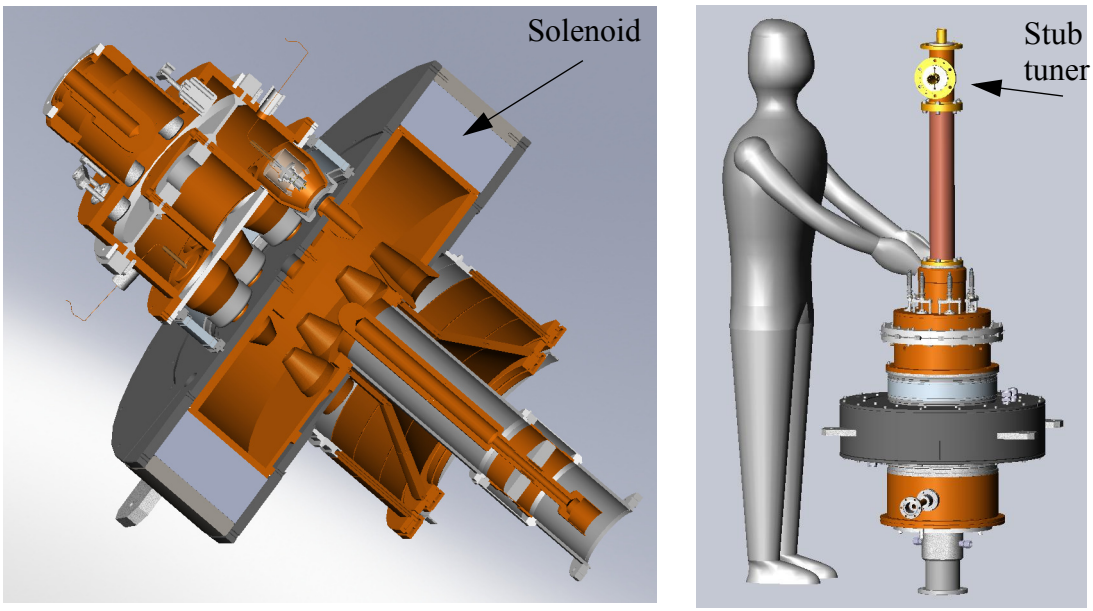

Figure 13. Solid model of the MBIOT. The left image is the seal-in assembly, which includes all vacuum sections. The right image includes the input waveguide (at the top). The human figure is 6 ft tall.

3. Fabrication

All parts were received by February 2011. Problems at the vendor's site resulted in an eighteen month delay in delivery. The other major item is the RF driver, which was delivered in August 2010. Assembly is proceeding and scheduled for completion by April 2012.

3.1. Input Cavity

Figure 14 shows the current status of the input cavity assembly.The stainless steel tubes around the periphery are the power inputs for the electron guns. The electron guns will be mounted in the large, partially visible, holes in the base plate.

Figure 15 shows three of the header assemblies for the electron guns and the insulator plate for the input cavity. Recall that the input cavity is at atmospheric pressure;

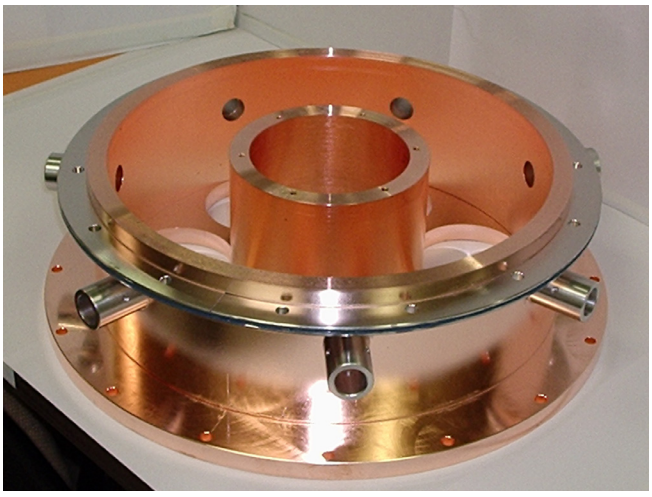

Figure 14. Input cavity

however, the RF input is at ground potential, while the cavity wall with the electron guns is at - 30 kV. The teflon plate provides the voltage isolation.

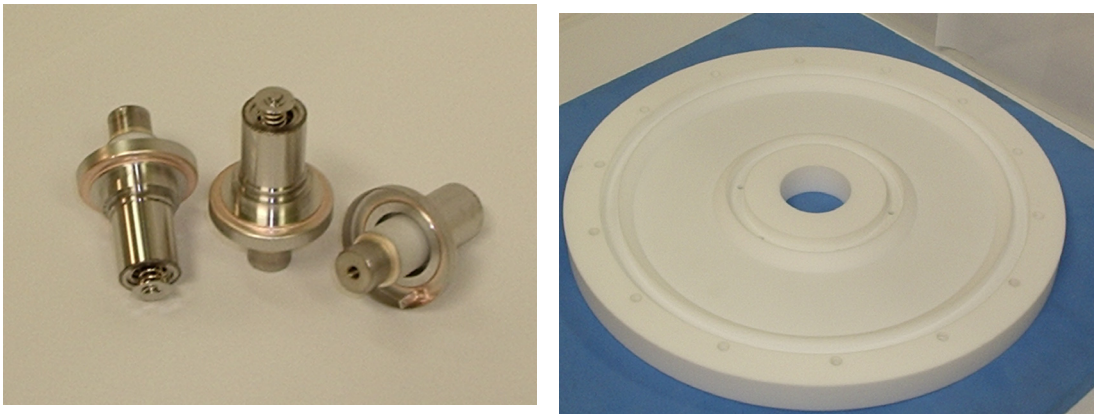

Figure 15. The left image shows three of the seven headers used for power connections to the electron guns. The right image is the teflon insulator plate for the input cavity.

3.2. Diode Region and Beam Line

Figure 16 shows the high voltage vacuum ceramic assembly that separates the input cavity form the output cavity. Also shown is one of the anodes, along with one set of the output cavity nose sections.

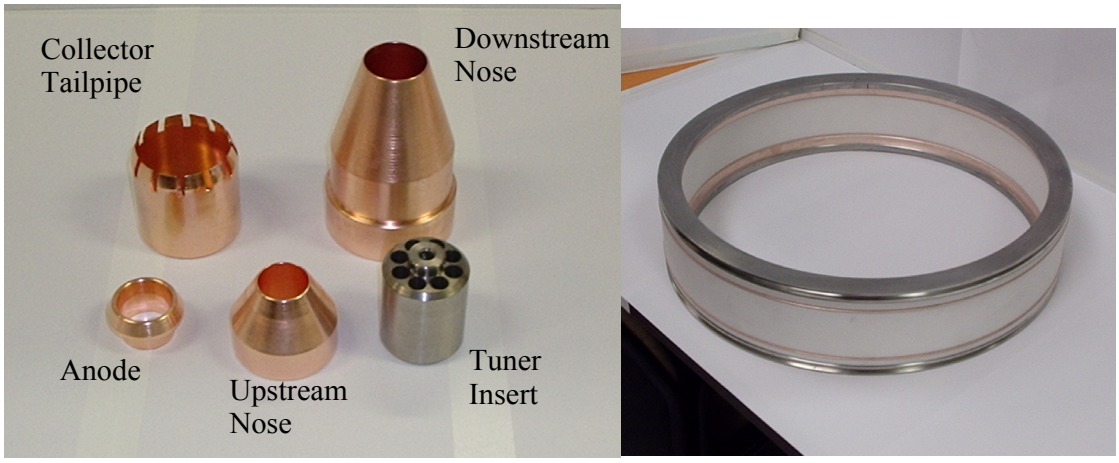

Figure 16. Left photo shows various components along the a beam line. The right image is the high voltage ceramic assembly

3.3. Output Cavity

Figure 17 shows parts for the output cavity. The iron plates are brazed to the copper end plates of the cavities. Water flows between the brazed plates for cooling.

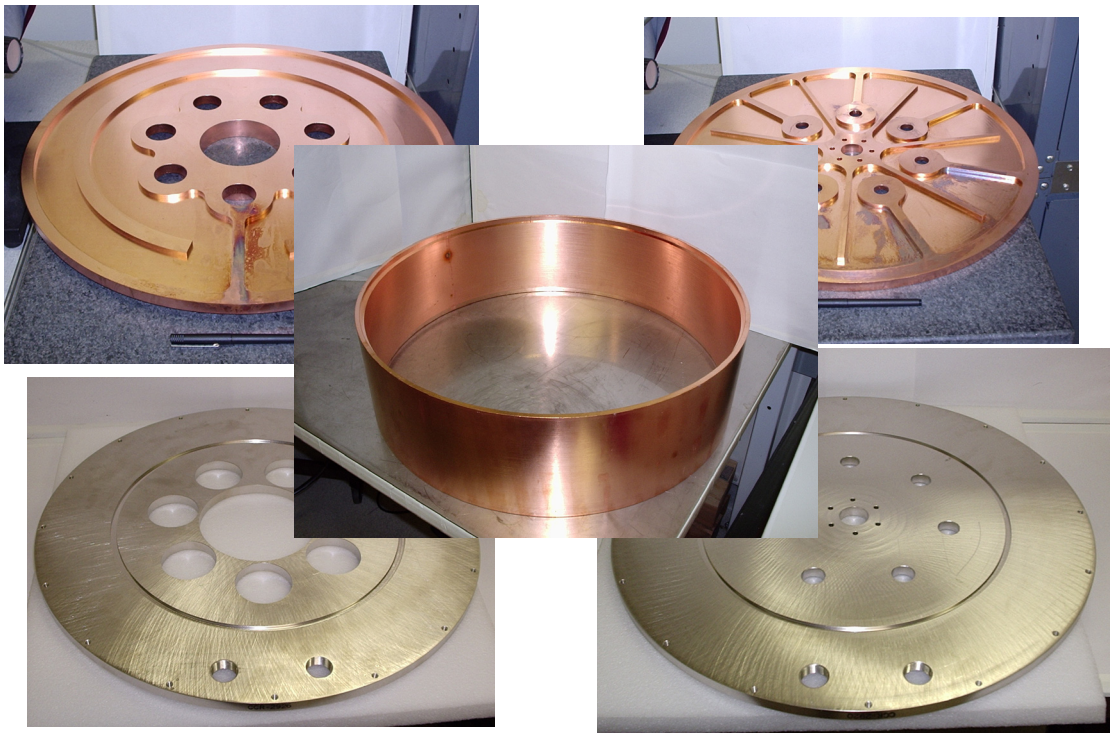

Figure 17. Output cavity end wall and outer wall cylinder. The end walls contain cooling channels sealed by the input and output polepiece

3.4. Output coupler and window

The output window is completed and brazed to the base of the output coupler. This assembly will be completed at cold test, when the penetration depth of the output coupler will set the output cavity Q.

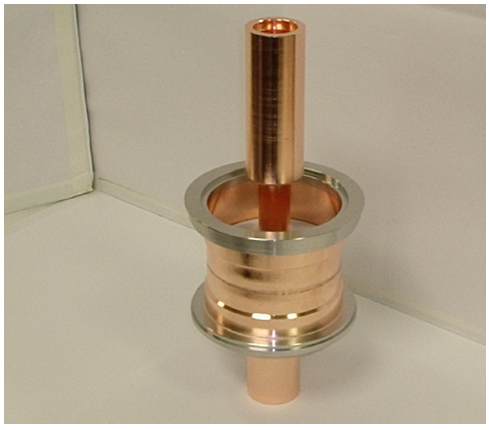

Figure 18. Output window and coupler

3.5. Collector

Figure 19 shows the two major subassemblies for the collector. The conical section forms the inner radius of the collector and the cylindrical cylinder forms the outer wall where most electrons impact.The ring-shaped parts interace the two assemblies and provide the water manfold for cooling.

Figure 19. Collector subassemblies and parts

3.6. Solenoid

Figure 20 shows a photo of the solenoid, which mounts around the output cavity.

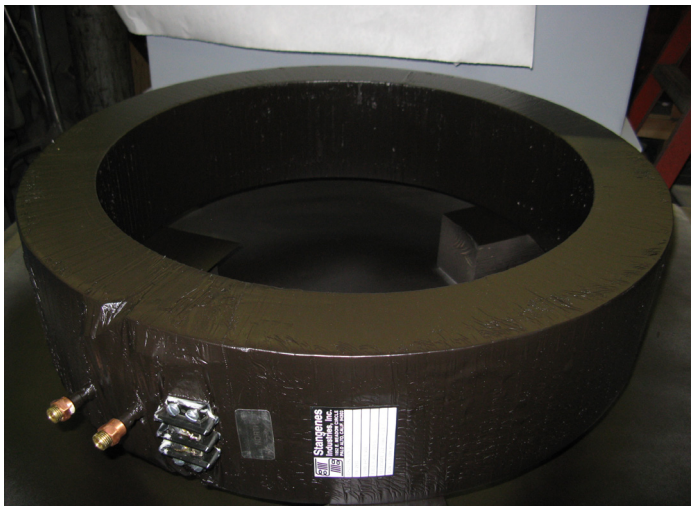

Figure 20. Solenoid

4. Schedule

Even though the Phase II program is concluded, CCR is continuing the MBIOT development using internal funds and additional funds provided by our industrial partner. Several major subassemblies remain to by built. Those with maximum risk include the brazing of the iron polepiece plates the the output cavity end wall plates. The differential thermal expansions will likely cause some distortion, so subassembly machining is planned correct for these. Other critical brazes include the weld rings to the collector and output cavity and the brazing of weld rings into the input cavity for welding the electron guns.

It is anticipated that the most critical brazes can be completed by the end of December 2011. Several additional months will be required to complete the seal-in assembly and bake the tube.

Testing will be performed at the Advanced Photon Source facility at Argonne National Laboratory (ANL). This is currently planned for spring 2012.

5. Summary

The Phase II program is concluded, but development of the MBIOT is continuing. A number of critical braze and welding processes remain to be completed, though much of the assembly is completed. The goal is the complete the assembly and test in 2013. It is anticipated that testing will continue at ANL to determine the potential implementation of these tubes in the next APS upgrade.